

Optical Engineering

OpticalEngineering.SPIEDigitalLibrary.org

Determination of thermal diffusivity of opaque materials using the photothermal mirror method

Aristides Marcano
Gabriel Gwanmesia
Mark King
Daniel Caballero

Determination of thermal diffusivity of opaque materials using the photothermal mirror method

Aristides Marcano,^{a,b,*} Gabriel Gwanmesia,^b Mark King,^{a,b} and Daniel Caballero^{a,b}

^aDelaware State University, Optical Science Center for Applied Research, 1200 North DuPont Highway, Dover, Delaware 19901, United States

^bDelaware State University, Department of Physics and Engineering, 1200 North DuPont Highway, Dover, Delaware 19901, United States

Abstract. A pump-probe photothermal mirror (PTM) method has been developed to determine the thermal diffusivity of opaque solid samples. The method involves the detection of the distortion of a probe beam whose reflection profile is affected by the photoelastic deformation of a polished material surface induced by the absorption of a focused pump field. We have measured the time dependence of the PTM signal of Ti, Al, Cu, Sn, Ag, and Ni samples. We show theoretically and experimentally that the time derivative of the signal in the first microseconds is proportional to the square root of the thermal diffusivity coefficient. The method affords a simple calibration and efficient interpretation of experimental data for a sensitive determination of the thermal diffusivity coefficient for materials. We demonstrate the applicability of the technique by measuring the thermal diffusivities of wadsleyite (β -Mg₂SiO₄) and diopside (MgCaSi₂O₆), two important minerals relevant to geophysical studies. © 2014 Society of Photo-Optical Instrumentation Engineers (SPIE) [DOI: 10.1117/1.OE.53.12.127101]

Keywords: photothermal mirror; photothermal effects; determination of thermal diffusivity.

Paper 141443 received Sep. 16, 2014; accepted for publication Nov. 20, 2014; published online Dec. 8, 2014.

1 Introduction

The photothermal mirror (PTM) technique has already been developed to determine the thermal, optical, and mechanical properties of materials.^{1–8} This method is particularly important for characterizing opaque materials. The idea is based on the generation of nanometric surface distortions that result from the absorption of an excitation light of relatively high intensity. The surface distortions affect the reflected wavefront of a probe light used to test the PTM. The technique uses a probe beam with dimensions larger than the deformation area. In this regard, the method differs from previous photothermal deformation or photodeflection techniques which used a probe beam with a spot dimension much smaller than the deformation area and thus requiring more careful and accurate alignment of the pump and the probe beams.^{9–12} A useful signal can be generated by measuring the transmission of the reflected probe light through a small aperture located at some distance from the sample. The PTM signal is defined as the relative change of the probe light transmission through the aperture. In the continuous wave regime of excitation, the signal grows as the square root of time in the first microseconds after the start of illumination. The signal reaches a stationary value when thermal diffusivity equilibrates the intake of thermal energy, yielding stationary values for the induced thermal gradients. The steady state situation is reached within a few milliseconds for metals, whose thermal diffusivities based on the simultaneous resolution of the thermoelastic equation for the surface deformations range from 10^{-5} to 2×10^{-4} m² s⁻¹. The theoretical model used to explain the PTM method is based on the simultaneous resolution of the thermoelastic equation for the surface deformations and the heat conduction equation. The thermal surface deformation yields a phase shift of

the reflected probe beam of light. Diffraction theory provides the value of the probe wavefront at the detector location. The method affords a simple nondestructive determination of the photothermal properties of the sample.

In this work, we have developed a simple and practical PTM technique to measure the thermal diffusivity of opaque samples. Based on the developed theoretical model for the PTM effect, we numerically show that the time derivative for the first microseconds of growth of the PTM signal divided over its stationary value is linearly proportional to the square root of the thermal diffusivity coefficient. We have studied the time dependence of the PTM signal for six different metals: Ag, Cu, Ni, Al, Sn, and Ti. By measuring the time derivatives of these dependences, we demonstrate the validity of the theoretical predictions. We provide a calibration curve of the values of the time derivatives of the PTM signal that we have subsequently used to determine the thermal diffusivities of wadsleyite (β -Mg₂SiO₄) and diopside (MgCaSi₂O₆), two important minerals relevant to geophysical studies.

2 Theoretical Consideration

We consider a Gaussian beam of radius a , which impinges over a flat reflective surface of a semi-infinite sample at a small angle of incidence. The absorption in the sample generates a distortion or “bump” of the surface due to the photoelastic effect.² A second Gaussian probe beam of light is directed toward the surface distortions. The spot radius a_p of the probe beam is much larger than a but is still small compared with the sample dimensions. The distortions affect the phase of the reflected wave, resulting in defocusing of the reflected probe beam at the far field. To describe the PTM effect, we use the model developed by Astrath et al.^{1–8} This model is based on the simultaneous resolution of the equations for temperature changes $T(r, z, t)$ and surface

*Address all correspondence to: Aristides Marcano, E-mail: amarcano@desu.edu

displacements $\vec{u}(r, z, t)$ given in Eqs. (1) and (2), as functions of transversal coordinate r , longitudinal coordinate z , and time t :

$$(1 - 2\nu)\nabla^2\vec{u} + \nabla \cdot (\nabla \cdot \vec{u}) = 2(1 + \nu)\alpha_T\nabla T, \quad (1)$$

$$\frac{\partial}{\partial t}T - D\nabla^2T = \frac{\psi\alpha I(r, t)}{C_p\rho}, \quad (2)$$

where ν is the Poisson ratio, α_T is the thermal expansion coefficient, D is the sample's thermal diffusivity coefficient, C_p is the specific heat, ρ is the density, α is the absorption coefficient, and ψ is the fraction of absorbed energy converted to heat, and

$$I(r, t) = \begin{cases} 0, & \text{if } t < 0 \\ \frac{2P_e}{\pi a^2} \exp\left(-\frac{r^2}{a^2}\right) & \text{if } t \geq 0 \end{cases}, \quad (3)$$

where P_e is the power of the excitation beam. Cylindrical coordinates with axial symmetry have been chosen because of the symmetry of the Gaussian excitation beam. We consider the initial conditions $T(\infty, z, t) = 0$ and $T(r, z, 0) = 0$, and the boundary conditions at a free surface $\sigma_{rz}|_{z=0} = \sigma_{zz}|_{z=0} = 0$, where σ_{rz} and σ_{zz} are the normal stress components.⁶ The displacement in the direction of z generates a phase shift in the reflected probe beam, which can be written as³

$$\Delta\Phi = \frac{2\pi}{\lambda_p} \{[u_z(r, 0, t) - u_z(0, 0, t)]\}, \quad (4)$$

where λ_p is the probe light wavelength. Using Eqs. (1) and (2), Sato et al. have obtained the following solution for the phase shift $\Delta\Phi$ for a semi-infinite sample under the conditions of high absorption³ given by

$$\Delta\Phi(g, t) = \Delta\Phi_0 \int_0^\infty \exp(-\eta^2/8) f(\eta, t) J_0(\eta\sqrt{gm}) d\eta, \quad (5)$$

where

$$f(\eta, t) = (\eta t/t_c) \text{Erfc}\left[\eta\sqrt{t/(4t_c)}\right] - 2\sqrt{t/(\pi t_c)} \exp[-\eta^2 t/(4t_c)] + 2\text{Erf}\left[\eta\sqrt{t/(4t_c)}\right]/\eta. \quad (6)$$

J_0 represents the Bessel function of the zeroth order, $\text{Erf}(x)$ is the error function and $\text{Erfc}(x)$ is the complementary error function, $\Delta\Phi_0 = -P_e\psi\alpha_T(1 + \nu)/(\lambda_p\kappa)$ measures the amplitude of the PTM effect, κ is the sample's thermal conductivity, $g = (r/a_p)^2$, $m = (a_p/a)^2$, and $t_c = a^2/(4D)$ is the thermal mirror build-up time. The probe field at the detector position can be calculated using the diffraction theory in a similar way to the method carried out for the thermal lens effect in a transmission experiment.¹³⁻¹⁵

We have calculated the value of the probe field amplitude at the center of the probe beam spot at the detector plane ($r = 0$). This corresponds to the situation of using an

aperture much smaller than the probe beam spot and placed at the center of this spot. The probe light power transmitted through the aperture can be then written as^{13,14}

$$I(t) = I_0 \left| \int_0^\infty \exp[-(1 + iV)g - i\Delta\Phi(g, t)] dg \right|^2, \quad (7)$$

where I_0 is a constant and $V = z_p/z_0 + z_0[(z_p/z_0)^2 + 1]/d$, z_p is the distance between the probe beam waists to the sample, z_0 is the Rayleigh range of the probe beam, and d is the distance from the sample to the detection plane. We define the signal as the relative change of probe light power transmitted through the aperture

$$S(t) = \frac{I(t) - I(0)}{I(0)}. \quad (8)$$

According to Eq. (4), the induced phase shift provides information about the spatial displacement profile. The surface deformation has been estimated on the order of few nanometers.² The information about the spatial profile is basically lost when performing the integration over the surface of the PTM [see Eq. (7)] that provides the intensity of the probe beam for only one point at the detection plane. However, this information can be recovered by monitoring the probe intensity for all points of the probe beam spot at this plane using a CCD camera instead of only one aperture. The displacement profile generated by the PTM effect is basically the two-dimensional Fourier transform of the diffraction spot of the probe field. The study falls beyond the scope of the present work which is mostly dedicated to the use of the PTM effect for practical determination of the thermal diffusivity.

In Fig. 1(a), we show the PTM signal calculated using Eqs. (5)–(8) and parameters $z_p = 0$, $z_0 = 2$ m, $d = 0.1$ m, and $a = 4 \times 10^{-5}$ m. We have expressed the signal in units relative to the stationary value. The time is given in units of the time t_c . The signal exhibits two distinctive time regimes. For times smaller than $100 t_c$, the signal grows rapidly. A detailed study shows that the signal grows as the square root of the time. For times much larger than $100 t_c$, the signal enters a stationary regime. Under this condition, the thermal diffusivity equilibrates the intake of energy to the point that the surface deformation does not change in shape. For values of diffusivity between 0.1 and $2 \times 10^{-4} \text{ m}^2 \text{ s}^{-1}$, which are characteristics of metals, we estimate t_c to be in the range of 2 to $40 \mu\text{s}$.

The results confirm that in metals, the stationary regime is reached in the time frame of milliseconds. In Fig. 1(b), we have plotted the normalized signal calculated numerically as a function of the square root of time for the first $100 \mu\text{s}$. The calculation has been performed for three diffusivity values: 0.1 , 0.6 , and $2 \times 10^{-4} \text{ m}^2 \text{ s}^{-1}$. We numerically show that the slope of this dependence provides the value of thermal diffusivity. Figure 1(c) shows that the calculated slope is a linear function of the square root of the thermal diffusivity. Experiments described below confirm the predictions of the theoretical model.

3 Experimental Approach

Figure 2 is a schematic diagram of the pump-probe PTM spectrometer that we have developed to study the time

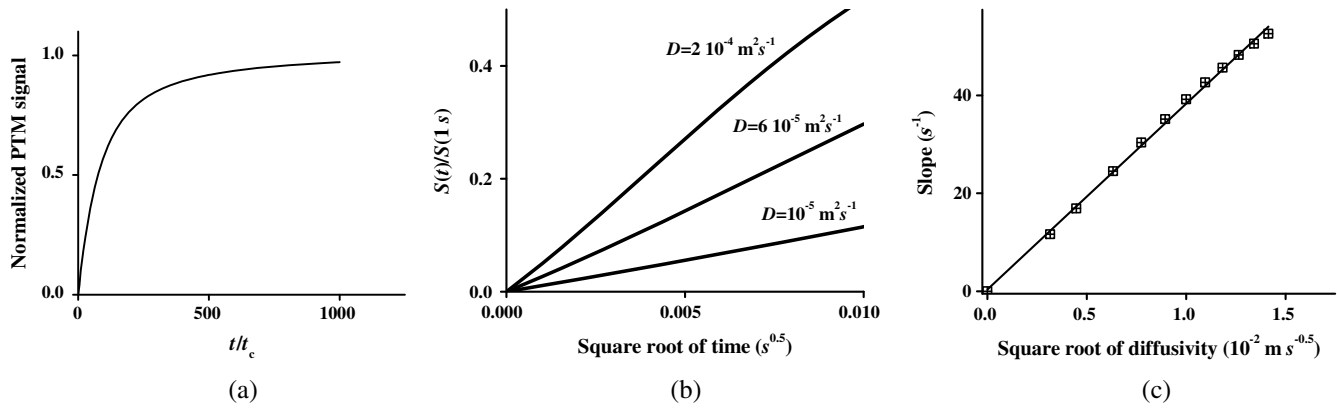


Fig. 1 (a) Photothermal mirror (PTM) signals calculated using Eqs. (5)–(8) and parameters $z_p = 0$, $z_o = 2 \text{ m}$, $d = 0.1 \text{ m}$, and $a = 4 \times 10^{-5} \text{ m}$. (b) Normalized PTM signals as a function of the square root of time for three $D = 0.1, 0.6$, and $2 \text{ cm}^2 \text{ s}^{-1}$ as indicated. (c) Values of the slope of the plots similar to those shown in (b) as a function of the square of diffusivity calculated for 11 different values of thermal diffusivity.

dependence of the PTM signal. A diode-pumped Nd-YAG laser (Lasever LSR 532 NL) generating at its second harmonic (532 nm) provides a 750-mW pump beam. Using the mirror M_1 and the focusing lens FL (15-cm focal length), the light is focused onto the sample forming an angle $\beta = 7.5 \text{ deg}$ with respect to the normal of the sample's surface. A glass plate B_1 deviates about 4% of this light toward a reference detector. The reflected pump light is blocked using a beam trap D. The pump light is modulated electronically using the signal generator SG (G^W Instek GFC 3015). Modulation frequencies between 10 and 50 Hz have been used for the samples in this study. A 2 mW He-Ne laser provides the probe light at 632 nm. Using lens M_2 , the light is directed perpendicularly, without focusing toward the sample centered at the focal point of the pump beam. The diameter of the probe beam spot at the sample is estimated as 1 mm. This spot is much larger than the spot radius of the pump field estimated to be $30 \mu\text{m}$. A small glass plate B_2 redirects a fraction of the reflected probe light to the aperture A using mirror M_3 . A negative lens DL (-3-cm focal length) defocuses the reflected probe light to ensure that

its spot beam radius is at least 10 times larger than the aperture radius. A semiconductor detector S measures the current transmitted through the aperture probe light power. The photocurrent generated by this detector is amplified by a current amplifier (Stanford Research Systems SR) and then sent to a digital oscilloscope (Tektronix TDS 3052) for data processing and collection.

We use a noncollinear scheme, where the pump and probe beam describe different paths. The scheme facilitates the alignment procedure and precludes parasitic signals from the pump light from entering the detector. The value of the angle β can affect the final value of the signal. However, this effect is small. The pump beam spot surface changes only slightly by changing the angle β . Additionally, the diameter of the PTM is about 10 times larger than the pump spot diameter.² The spot dimension of the probe is about 50 times larger than the spot diameter of the pump field. Under this geometry, the pump beam affected area can be considered nearly a spatial point compared with the spatial dimensions of the PTM and with the spot dimension of the probe beam. Small changes in the spot surface of the pump field should not substantially

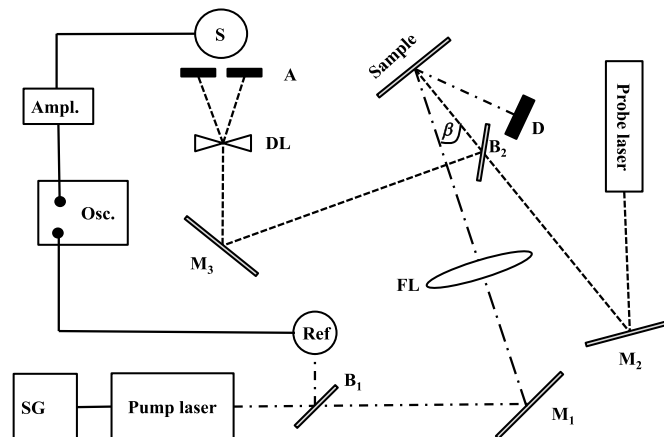


Fig. 2 Schematic diagram of the experimental setup consisting of a pump laser (DPPS Nd-YAG, 750 mW at 532 nm) whose modulation frequency is controlled by the signal generator SG, a probe laser (He-Ne), beam-splitters B_1 and B_2 , mirrors M_1 , M_2 , and M_3 , a beam trap D, a focusing lens FL, a defocusing lens DL, an aperture A, a reference detector Ref, a signal detector S, a current amplifier (Ampl.), and a digital oscilloscope (Osc.).

affect the value of the signal. We have changed the angle of incidence of the pump beam β from 7.5 deg to 21 deg and have found no change in the signal's amplitude within an experimental error of 3% in agreement with this prediction. We have maintained the same angle of incidence $\beta = 7.5$ deg in all experiments described in the work.

In view of the fact that the probe beam is larger than the PTM, speckle or interference effects can take place due to changes in the path length from adjacent points on the surface and may affect the reflected probe beam spot at the far field. However, these effects are automatically corrected by the way the signal is calculated [see Eq. (8)]. The signal is proportional to the relative change of the probe light transmission. Parasitic interference affects the probe wavefront in the presence and absence of the pump beam in a similar way. By taking the relative change of the transmission, these effects are substantially reduced.

4 System Calibrations

We have calibrated the system using metallic samples whose thermal diffusivity values are well known. The samples are Cu, Al, Ni, Ti, and Sn, in the form of metallic plates of about a 2-mm thickness about 4-mm diameter whose surfaces have been polished to an optical reflecting finish using 9-, 6-, 3-, and 1- μm diamond pastes in succession. For the purpose of the analysis, the samples can be considered semi-infinite in the coordinate perpendicular to the plate surface and infinite in the radial direction. In Table 1, we show the thermal conductivity, density, and heat capacity values of Ti, Ni, Sn, Al, and Cu published elsewhere.¹⁶ We have calculated the thermal diffusivity coefficients of the metals using these parameters and the equation $D = \kappa/(\rho C_p)$ (see column 5 in Table 1). We first measured the transmission of the probe light as a function of time for each sample. The signal is then calculated using Eq. (8). A stationary value is achieved by registering the signal for a relatively long time (usually few milliseconds) and for times smaller than 1 ms, the values of the signal are divided over the stationary value and produce plots of the normalized value as a function of the square of time. Linear dependence is obtained for relatively small times of up to 100 μs . Finally, we show that the slopes of these plots are proportional to the thermal diffusivity values of the metallic samples.

Table 1 Thermal conductivity, density, heat capacity, and calculated thermal diffusivity values of the metallic samples used in this study.

Sample	Thermal conductivity ($\text{W m}^{-1} \text{K}^{-1}$)	Density (kg m^{-3})	Heat capacity ($\text{J kg}^{-1} \text{K}^{-1}$)	Thermal diffusivity ($\text{m}^2 \text{s}^{-1}$)
Ti	21.9	4510	522	9.30×10^{-6}
Ni	97.5	8908	445	2.46×10^{-5}
Sn	66.6	7260	227	4.04×10^{-5}
Al	237	2700	897	9.78×10^{-5}
Cu	401	8960	384	1.16×10^{-4}

5 Results and Analysis

In Fig. 3, we show the time dependence for Ti, Sn, and Ni. Similar results have been obtained for the rest of the samples. The pump light has been set to start at $t = 0$ and stays on for 20 ms. All signals exhibit a rapid growth during the first microseconds of the experiment. As predicted by the model, the signals start reaching stationary values a few milliseconds after the start of the irradiation. As expected, the magnitude of the signal and their velocity of growth over time are different for each material because of their unique properties and different thermal diffusivity values. By normalizing the signal to its stationary value, we obtain only the contribution related to thermal diffusion effects.

In Fig. 4, we show the normalized values over the stationary values' signal as a function of the square of time. As predicted by the model, the dependence is linear up to 200 μs . The slopes of the lines correspond to the thermal diffusivities.

In Fig. 5, we show the slopes of the signal of each metallic sample as a function of the square of the diffusivity values taken from Table 1. The solid line is a linear least square fit of the experimental data. In agreement with the theoretical predictions, the data fit a linear dependence with a standard

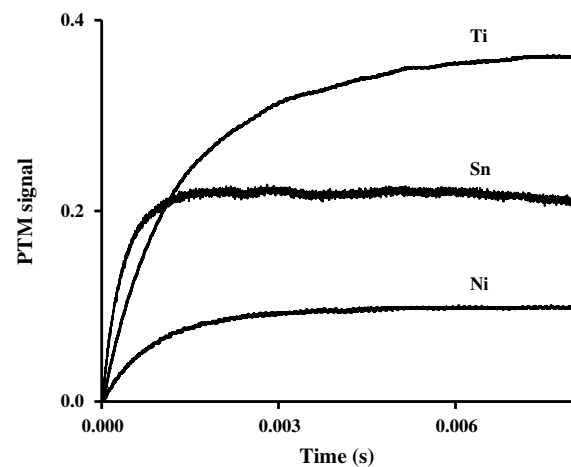


Fig. 3 Measured PTM signals for Ti, Sn, and Ni using 750 mW at 532-nm pump light.

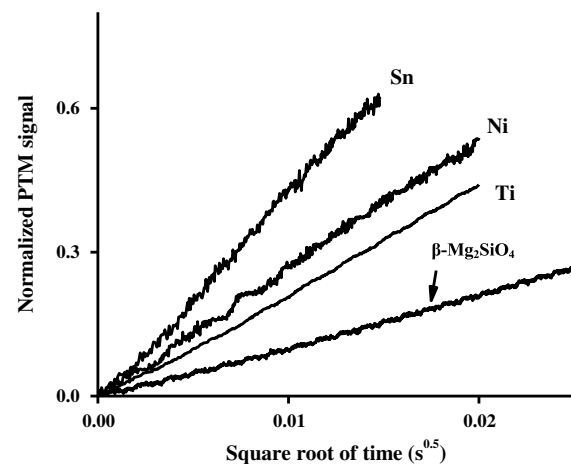


Fig. 4 Normalized PTM signals for Ti, Sn, and Ni and the mineral wadsleyite as a function of the square of time.

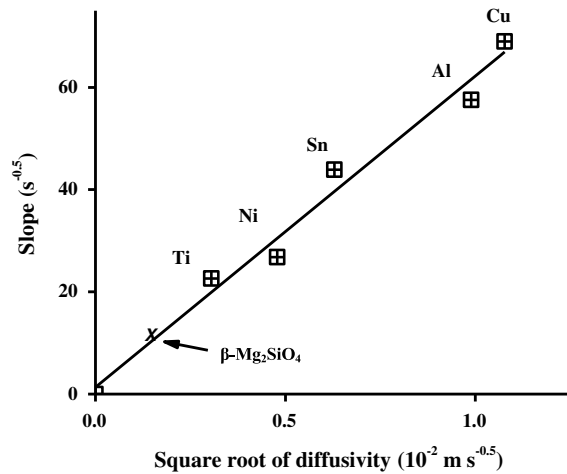


Fig. 5 Slopes of the plots similar to those shown in Fig. 4 for Ti, Ni, Sn, Al, and Cu as functions of the square of the diffusivity coefficient values taken from Table 1. The solid line is a linear least square fitting. We have added the results for the slope of the mineral wadsleyite, which allows the determination of its thermal diffusivity coefficient.

deviation of 4%. The calibrations obtained in this study can be used for the determination of thermal diffusivity values of other samples.

6 Technique Application

We have utilized the calibration to study the thermal diffusivities of wadsleyite ($\beta\text{-Mg}_2\text{SiO}_4$) and diopside ($\text{MgCaSi}_2\text{O}_6$), two important minerals relevant to geophysical studies. The data are important for understanding heat and material transports in the planetary interior. Wadsleyite ($\beta\text{-Mg}_2\text{SiO}_4$) is the high pressure polymorph of the Mg end-member of olivine [$(\alpha\text{-}(\text{Mg}, \text{Fe})_2\text{SiO}_4$] and is believed to be an abundant mineral in the Earth's upper mantle. Wadsleyite is the product of the transformation of olivine under high pressure and temperature conditions of the region between 410 and 670 km in the Earth, called the transition zone. In Fig. 4, we indicate the result of the analysis for the wadsleyite sample. From the analysis, we estimate a thermal diffusivity coefficient to be $(2.6 \pm 0.1) \times 10^{-6} \text{ m}^2 \text{ s}^{-1}$. Our results are in good agreement with previously published data obtained by an elaborated method based on direct measurement of temperature using thermocouples.^{17–19} We have also determined the thermal diffusivity of diopside ($\text{MgCaSi}_2\text{O}_6$), a silicate mineral found in most metamorphic rocks in the Earth's upper mantle, obtaining $D = (3.2 \pm 0.1) \times 10^{-8} \text{ m}^2 \text{ s}^{-1}$. Our result is also in good agreement with reported data on the mineral.²⁰

In our experiments, we have used thermoelastic materials with high light absorption coefficients such as metals and minerals. An important limitation of the method is that the sample must have a good reflecting surface. In general, any physical effect able to induce changes of the reflection coefficient can yield a signal. In this regard, the method can be applied to materials with good photothermal dependence of the reflection coefficient even if the photoelasticity effect is minimal. The PTM effect also requires a certain level of absorption. By careful selection of the excitation wavelength, it is possible to obtain an adequate absorption for a given required signal-to-noise ratio. On the other hand, the method is remarkably sensitive due to its intrinsic phase

character. Previous experiments have demonstrated the efficiency of the PTM technique for materials with low absorption.¹⁷ Thus, the developed PTM calibration method can, in principle, be applied to a variety of materials such as low-absorbing glasses, plastics, ceramics, semiconductors, and thin films, among other materials, provided a good quality reflection surface can be achieved on them.

7 Conclusions

We have developed a pump-probe PTM method for investigating the thermal diffusivity of opaque samples. We show theoretically and experimentally using five metallic samples that the signal depends linearly on the square root of the time in the first microseconds after the start of the excitation. The value of the slope of this dependence provides a simple way for the determination of the thermal diffusivity coefficient. We have used the method to measure the thermal diffusivity of Earth minerals, whose value is difficult to establish using more traditional methods based on direct monitoring of temperature changes.

Acknowledgments

Authors acknowledge the support of the National Science Foundation under Grants EAR-0810209 to GDG and of National Science Foundation CREST Grant No 1242067.

References

- N. G. C. Astrath et al., "Time-resolved thermal mirror for nanoscale surface displacement detection in low absorbing solids," *Appl. Phys. Lett.* **91**(19), 191908 (2007).
- L. Malacarne et al., "Nanoscale surface displacement detection in high absorbing solids by time-resolved thermal mirror," *Appl. Phys. Lett.* **92**(13), 131903 (2008).
- F. Sato et al., "Time-resolved thermal mirror method: a theoretical study," *J. Appl. Phys.* **104**(5), 053520 (2008).
- L. C. Malacarne et al., "Time-resolved thermal lens and thermal mirror spectroscopy with sample-fluid heat coupling: a complete model for material characterization," *Appl. Spectrosc.* **65**(1), 99–104 (2011).
- V. S. Zanuto et al., "Thermal mirror spectrometry: an experimental investigation of optical glasses," *Opt. Mater.* **35**(5), 1129–1133 (2013).
- N. G. C. Astrath et al., "Finite size effect on the surface deformation thermal mirror method," *J. Opt. Soc. Am. B* **28**(7), 1735–1739 (2011).
- G. V. B. Lukasiewicz et al., "Pulsed-laser time-resolved thermal mirror technique in low absorbance homogeneous linear elastic materials," *Appl. Spectrosc.* **67**(10), 1111–1116 (2013).
- O. S. Arestegui et al., "Combined photothermal lens and photothermal mirror characterization of polymers," *Appl. Spectrosc.* **68**(7), 777–783 (2014).
- M. Olmstead, N. M. Amer, and S. Kohn, "Photothermal displacement spectroscopy: an optical probe for solid and surfaces," *Appl. Phys. A* **32**(3), 141–154 (1983).
- A. Mandelis, "Absolute optical absorption coefficient measurement using transverse photothermal deflection," *J. Appl. Phys.* **54**(6), 3404–3409 (1983).
- J. C. Cheng and S. Y. Zhang, "Three dimensional theory to study photothermal phenomena of semiconductors. II. Modulated photothermal deflection," *J. Appl. Phys.* **70**(11), 7007–7013 (1991).
- D. P. Almond and P. M. Patel, "Photothermal science and techniques," in *Physics and Its Applications*, Vol. 10, p. 84, Chapman & Hall, London (1996).
- J. Shen, R. D. Lowe, and R. D. Snook, "A model for cw laser induced mode-mismatched dual-beam thermal lens spectrometry," *Chem. Phys.* **165**(2–3), 385–396 (1992).
- M. L. Baesso, J. Shen, and R. D. Snook, "Three dimensional model for CW laser-induced mode-mismatched dual-beam thermal lens spectrometry and time resolved measurements of thin-film spectra," *J. Appl. Phys.* **75**(8), 3738–3748 (1994).
- A. Marcano, C. Loper, and N. Melikechi, "Pump probe mode mismatched Z-scan," *J. Opt. Soc. Am. B* **19**(1), 119–124 (2002).
- D. R. Lide, *CRC Handbook of Chemistry and Physics*, 90th ed., CRC Press, Boca Raton, Florida (2009).
- Y. Xu et al., "Thermal diffusivity and conductivity of olivine, wadsleyite and ringwoodite to 20 GPa and 1373 K," *Phys. Earth Planet. Inter.* **143–144**, 321–336 (2004).

18. T. Katsura, "Thermal diffusivity of silica glass at pressures up to 9 GPa," *Phys. Chem. Miner.* **20**(3), 201–208 (1993).
19. T. Katsura, "Thermal diffusivity of olivine under upper mantle conditions," *Geophys. J. Int.* **122**(1), 63–69 (1995).
20. A. Suzuki and D. C. Rubie, "Thermal diffusivity of diopside-composition glass at high temperature," in *Abstract # 11695, EGS-AGU-EUG Joint Assembly*, Nice, France (2003).

Aristides Marcano received his master's degree in physics with honors from M. V. Lomonosov Moscow State University, in Moscow, Russia, in 1977, and doctor of philosophy in physics and mathematics from the same university in 1980. He is currently a professor and chair of the Department of Physics and Engineering at Delaware State University. His main areas of interest are photothermal-induced phenomena, Z-scan, and optical and laser application in live sciences.

Gabriel Gwanmesia received his BS degree in physics and mathematics from Delaware State University in 1985. He received his MS degree in geophysics from the State University of New York,

Stony Brook, New York, USA, in 1987, and the PhD degree in geophysics from the same university in 1991. He is currently a professor of physics of the Department of Physics and Engineering at Delaware State University. He has been lately working in characterization of minerals using acoustic and thermal methods.

Mark King received his BS degree in engineering physics with a mathematics minor at Delaware State University in May 2013. He is currently a graduate student of the MS program in applied optics in the same university. His current graduate research is centered on pump-probe photo-thermal mirror techniques to determine the thermal diffusivity of solids.

Daniel Caballero is an undergraduate student of the BS program of the Department of Physics and Engineering at Delaware State University. He is currently interested in the use of the photothermal method for characterization of materials.